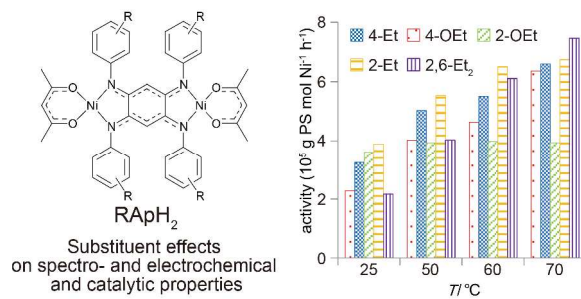




Dinuclear nickel(II) complexes with 2,5-diamino-1,4-benzoquinonediimine ligands as precatalysts for the polymerization of styrene: electronic and steric substituent effects

Journal:	<i>Dalton Transactions</i>
Manuscript ID:	DT-ART-09-2014-002858.R1
Article Type:	Paper
Date Submitted by the Author:	17-Oct-2014
Complete List of Authors:	Ohno, Keiji; Saitama University, Department of Chemistry, Graduate School of Science and Engineering Nagasawa, Akira; Saitama University, Department of Chemistry, Graduate School of Science and Engineering Fujihara, Takashi; Saitama University, Comprehensive Analysis Center for Science

Substituent effects by electron-donating ability and bulkiness of R in $[\{\text{Ni}(\text{acac})\}_2(\mu\text{-RAPH}_2)]$ (RAPH₂: azophenines) on properties and catalytic activity are reported.



ARTICLE

Dinuclear nickel(II) complexes with 2,5-diamino-1,4-benzoquinonediimine ligands as precatalysts for the polymerization of styrene: electronic and steric substituent effects

Cite this: DOI: 10.1039/x0xx00000x

Received 00th January 2012,
Accepted 00th January 2012

DOI: 10.1039/x0xx00000x

www.rsc.org/

Keiji Ohno,^a Akira Nagasawa,^a and Takashi Fujihara*^b

Catalytic polymerization of styrene with a series of dinuclear nickel(II) complexes [$\{\text{Ni}(\text{acac})\}_2\{\mu\text{-C}_6\text{H}_2\text{-}(\text{N-Ph-R})_4\}$] (R = 4-Et (**1a**), 4-OEt (**1b**), 2-OEt (**1c**), 2-Et (**1d**), and 2,6-Et₂ (**1e**)) in the presence of methylaluminoxane was studied under various conditions to evaluate the substituent effect. The activity of **1a–1e**, except **1c**, increased with an increase in the reaction temperature, and the highest activity (7.46×10^5 g PS mol⁻¹ Ni h⁻¹) was obtained using **1e** at 70°C. The electronic and steric properties of the ligand influenced on the activity at room temperature, 50°C, and 60°C; steric factors barely, whereas electronic factors slightly dominated the activity at 70°C. The activity with **1c** remained constant at all temperatures, probably due to the masking of the active center by the formation of inactive *N,N',O*-chelate species. The obtained polymers were atactic polystyrenes with molecular weights and molecular weight distributions in the range of 15000–43400 and 1.71–2.14, respectively. While a clear dependence of the molecular weight and molecular weight distribution on the temperature was observed, no significant dependence on the substituent was noted.

Introduction

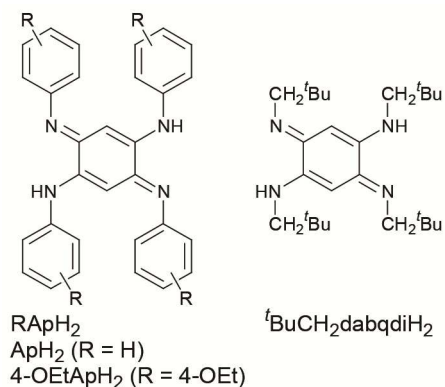
The discovery of Ziegler–Natta catalysts based on titanium chlorides and aluminum alkyls or chloride¹ triggered many studies on the catalytic polymerization of various monomers with early transition metal complexes.² In particular, the polymerization of styrene is of much interest because it is one of the few monomers polymerized by all of the known polymerization mechanisms (radical, cationic, anionic, and coordinated mechanisms), and polystyrene can be obtained with any one of three different stereo regularities (isotactic, syndiotactic, and atactic structures). For catalytic polymerization with late transition metal complexes, Brookhart synthesized precatalysts consisting of mononuclear Ni^{II} or Pd^{II} complexes with α -diimine chelating ligands in 1995.³ These complexes when activated by aluminum alkyl activators, such as methylaluminoxane (MAO), exhibited high catalytic activities for the polymerization of α -olefins. Since the initial report, many mononuclear complexes have been synthesized as precatalysts, and the effects of the bulkiness of the ligand backbone, the complex nuclearity, and the nature of the cocatalyst on their activities and the generated products have been investigated.⁴

Catalytic polymerization with dinuclear complexes has also been explored.^{4i,5} Such complexes were expected to exhibit different activities and provide polymers with different molecular weights compared to those obtained using

mononuclear analogues due to the cooperative effects between the two active centers. Osakada *et al.* reported that a double-decker-type dinuclear Ni complex exhibited high activity and provided a polymer with a different microstructure compared to that of the polymer obtained using a mononuclear analog.⁶ Recently, the catalytic activities of dinuclear Ni^{II} complexes with π -conjugated bridging ligands have been investigated. These complexes exhibited either activities twice those of their mononuclear analogs⁷ or an increased lifetime compared to that of their mononuclear analogs.^{4r}

Azophenine derivatives (RAPH₂, Scheme 1) are bridging and chelating ligands with two π -systems inside each of two N–C–C–C–N moieties. Although RAPH₂ compounds have been known for a long time, *e.g.* ApH₂ and 4-OEtApH₂ were synthesized in 1875 and 1984,⁸ respectively, the first complex with one of these ligands, a mononuclear Cu^I complex, was reported by Kaim *et al.* in 1998.⁹ After that initial report, other complexes of RAPH₂ and related compounds were synthesized,¹⁰ and the coordination chemistry of these metal complexes has been investigated.¹¹ In particular, multinuclear complexes have attracted much attention because of their potential applications in molecular devices that utilize the electronic communication between the metal centers through the delocalized π -conjugated systems in the N–C–C–C–N moieties. Notably, a one-electron reduced dinuclear Fe^{II} complex with ApH₂ exhibited the strongest magnetic exchange coupling ever observed in a single-molecule magnet.^{11k} Braunstein *et al.* and Jin *et al.* also respectively reported that

dinuclear Ni^{II} and Cu^{II} complexes with RApH₂ exhibited catalytic activity for the oligomerization and polymerization of ethylene, methyl methacrylate, and norbornene in the presence of AlEtCl₂ or MAO.^{11e,11g} Recently, we described the syntheses, structures, and properties of 4-EtApH₂ and its diprotonated species, as well as bis(boron difluoride), mononuclear and dinuclear Ni^{II} (**1a** and **2a**, respectively), and dinuclear Ir^{III} complexes, and also evaluated the effect of coordination to Lewis acids on the π -systems.¹²



Scheme 1 Azophenine derivatives (RApH₂), and ^tBuCH₂dabqdiH₂.

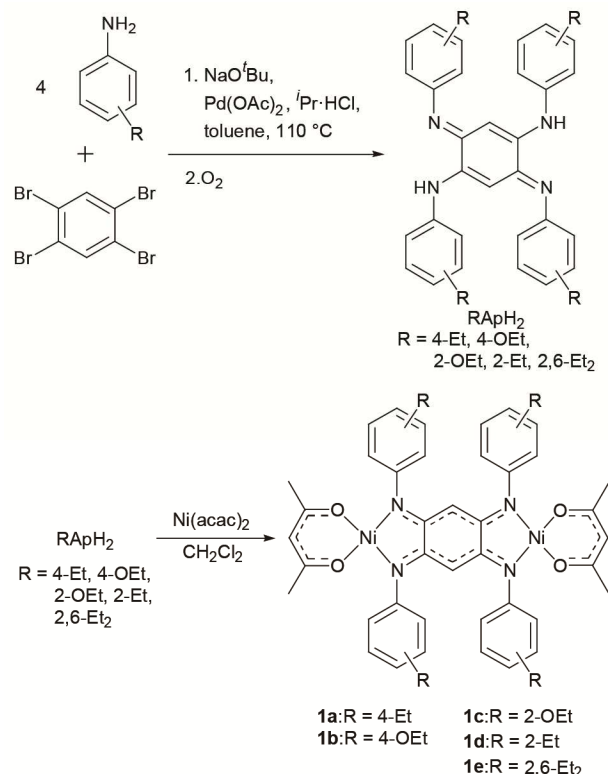
The electronic fine tuning of complexes using electron-donating and electron-withdrawing ligands is important for the development of molecular devices and polymerization catalysts, which are affected by the electronic communication between the metal centers and the nuclearity of the complexes, respectively. For example, a comparison of the redox properties of dinuclear Ni complexes with π -acceptable ApH₂ and σ -donable ^tBuCH₂dabqdiH₂ ligands (Scheme 1) revealed that the properties of the *N*-substituents influence the electronic states of the metal centers.^{11d}

Therefore, we proposed that dinuclear Ni complexes with RApH₂ ligands should enable the electronic fine tuning of the complexes as polymerization catalysts through the variation of the electron-donating ability of R (nitrogen substituent). In this study, we first synthesized four RApH₂ (R = 4-OEt, 2-OEt, 2-Et, and 2,6-Et₂), the dinuclear Ni^{II} complexes [$\{\text{Ni}(\text{acac})_2\}_2\{\mu\text{-RAp}\}$] (R = 4-OEt (**1b**), 2-OEt (**1c**), 2-Et (**1d**), and 2,6-Et₂ (**1e**)), and the mononuclear Ni^{II} complex [Ni(2-OEtApH₂)₂](ClO₄)₂ (**2c**) (Scheme 2). The effect of the substituent R on the structures and properties of the complexes was investigated. Furthermore, the polymerization of styrene with **1a–1e** in the presence of MAO was performed, and the influence of the electronic and steric properties of the substituent R on the catalytic activity, molecular weight (*M_w*), and molecular weight distribution (*M_w*/*M_n*) of the obtained polystyrene products was evaluated.

Results and Discussion

Syntheses and Characterization

The dinuclear Ni^{II} complexes [$\{\text{Ni}(\text{acac})_2\}_2\{\mu\text{-RAp}\}$] (R = 4-Et (**1a**),¹² 4-OEt (**1b**), 2-OEt (**1c**), 2-Et (**1d**), and 2,6-Et₂ (**1e**)) were prepared according to the method reported in the literature.¹² The mononuclear complex **2c** was synthesized by the reaction of 2-OEtApH₂ with Ni(ClO₄)₂·6H₂O (Scheme 2).



Scheme 2 Syntheses of ligand (RApH₂), dinuclear Ni^{II} complexes (**1a–1e**), and mononuclear Ni^{II} complex (**2c**).

The ¹H NMR spectra of the RApH₂ ligands in CDCl₃ showed resonances for the N–H and C₆–H₂ (ethyldine) protons of the diaminoquinonodiimine moiety in the range of δ 8.11–8.70 and 4.61–6.25, respectively. The spectra for complexes **1b–1e** in CDCl₃, however, showed no N–H resonances, suggesting that the deprotonated species, RAp²⁻, coordinates to the Ni centers to form these dinuclear complexes. In addition, the resonances for the C₆–H₂ protons of **1b–1e** were shifted upfield from those of the corresponding ligands because of an increase in the ring current effect of the *N*-phenyl rings, which in the complexes are locked perpendicularly to the central six-membered ring both in solution and in the solid state.¹²

The UV–vis absorption spectra of the RApH₂ ligands in CH₂Cl₂ showed strong absorption bands in the range of 355–438 nm, which are assigned to the π – π^* transition in the benzoquinonediimine moiety (Table 1). The spectra for complexes **1b–1e** in CH₂Cl₂ also showed two strong π – π^* transitions in the benzoquinonediimine moiety and metal ligand charge transfer (MLCT) absorptions in the range of 500–600 nm (Table 1).

In the cyclic voltammograms of complexes **1b–e** (in anhydrous CH₂Cl₂, NBu₄PF₆ as supporting electrolyte), two redox waves were commonly observed and assigned to two successive one-electron oxidation processes, *i.e.* Ni^{II}₂/Ni^{III}Ni^{III} and Ni^{II}Ni^{III}/Ni^{III}₂ (Table 1). The wider separation of the first and second oxidation processes for **1e** compared to those for **1a–d** may be induced by the higher planarity of the two π -conjugated systems in the N–C–C–N moieties than those of others

because **1e** has high symmetry and rigidity due to the steric substituent effect.

Table 1. UV-vis absorption maxima (λ) and molar extinction coefficient ($\log \epsilon$) of RApH₂ and the complexes **1a–e** in CH₂Cl₂, and redox potentials (E) of complexes **1a–e** in anhydrous CH₂Cl₂ (0.1 M NBu₄PF₆).

Compound	absorption maxima λ/nm , ($\log \epsilon$)	redox potentials E/N vs Fc/Fc ⁺	
		Ni ^{II} /Ni ^{III}	Ni ^{III} /Ni ^{III} ₂
4-EtApH ₂ ^a	398(4.40)		
4-OEtApH ₂	438(4.30)		
2-OEtApH ₂	404(4.30)		
2-EtApH ₂	377(4.40)		
2,6-Et ₂ ApH ₂	355(4.56)		
1a ^a	520(4.63), 559(4.71)	0.09	0.71
1b	524(4.42), 563(4.52)	0.01	0.52
1c	518(4.34), 558(4.45)	0.11	0.76
1d	509(4.59), 548(4.69)	0.21	0.79
1e	512(4.50), 547(4.60)	0.21	1.10

^a Ref. 12.

Molecular structures

Red crystals of 2-OEtApH₂, 2-EtApH₂, and 2,6-Et₂ApH₂ and purple crystals of **1b**, **1c**, **1e**, and **2c** were obtained via the vapor diffusion of hexane into the solutions of the corresponding compounds in CH₂Cl₂ or CHCl₃. These molecular structures were determined by X-ray diffraction analysis (Figures 1, 2, S1, and S2). The crystallographic data are summarized in Table S1, and selected bond lengths and angles are listed in Table S2.

The bond lengths of 2-OEtApH₂ exhibit a bond alternation of single and double bonds in each of the two N=C–C=N zigzag-shaped moieties (Figure 1), suggesting a localization of π -electrons. All the atoms in the diaminobenzoquinonediimine moiety were located coplanarly. The C1–N1 and C2–N2 bond lengths correspond to the single and double bonds, respectively, and the C1–N1–C4 and C2=N2–C14 bond angles suggest that N1 and N2 are attributed to amine (sp^3) and imine (sp^2) nitrogen atoms, respectively. The C1–C3A and C2–C3 bond lengths correspond to the double and single bonds, respectively, and the C1–C2 bond is slightly longer than the C2–C3 single bond. Intramolecular hydrogen bonding N(1)–H(1)⋯N(2) was also observed (Table S3), and this interaction suggests the tautomerization between the amine and adjacent imine. The molecular structures of 2-EtApH₂ and 2,6-Et₂ApH₂ were similar to that of 2-OEtApH₂ (Figures S1A and S1B, respectively).

The neutral molecule **1c** adopted a square-planar coordination geometry around the Ni center with the delocalization of six π -electrons over each of the two N–C–C–N moieties (Figure 2A). The dianionic bis(chelate) ligand 2-OEtAp²⁻ bridged two {Ni(acac)}⁺ fragments to form a dinuclear unit. In the N–C–C–N moieties, the two C–C bonds had similar lengths of ca. 1.38 Å, which is approximately the average of the values for the C–C single and C=C double bonds in 2-OEtApH₂, and the two C–N bonds were similar at ca. 1.34 Å. On the other hand, the C1–C2 bond length was very similar to that of 2-OEtApH₂, which is considered to be a single bond. The Ni–N bond lengths were shorter than those of **2c**. These observations suggest an extension of the π -conjugated systems between the two metal centers. The crystallographic data for **1b** and **1e** showed similar molecular structures to that of **1c** (Figures S2A and S2A, respectively).

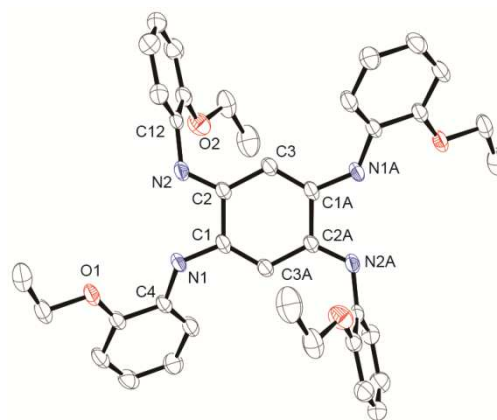


Fig. 1 Molecular structure of 2-OEtApH₂ with thermal ellipsoids at the 50% probability level. Hydrogen atoms are omitted for clarity.

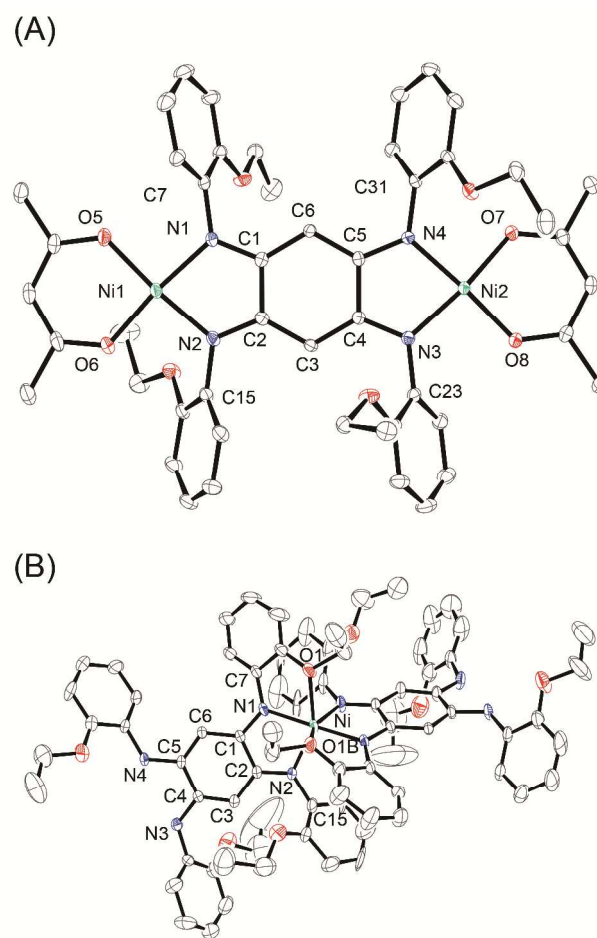
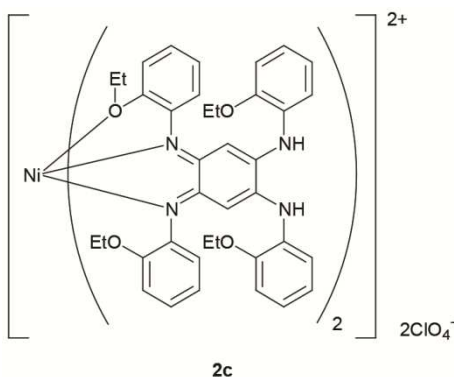


Fig. 2 Molecular structures of (A) **1c** and (B) **2c** with thermal ellipsoids at the 50% probability level. Hydrogen atoms and counter anions (ClO₄⁻) are omitted for clarity.

The mononuclear dication **2c** adopted a distorted octahedral bis(chelate) coordination geometry, with the Ni center coordinated with two N (imine) and one O (ethoxy) donors from each of two isomerized ligands (Figure 2B). The bond lengths in the N=C–C=N moieties also suggest an isomerization from the *para*-benzoquinonediimine of the free ligand to the *ortho*-benzoquinonediimine form in the complex

(Schemes 3). The Ni–N bond length (1.980 Å and 2.019 Å), the C–N(imine)–C bond angles (127.2° and 123.1°), and the N–Ni–N bite angle (80.49°) were shorter and wider than those of **2a** (2.073(2)–2.104(6) Å, ca. 119°, and ca. 77.8°, respectively),¹² probably due to a decrease in the intramolecular steric repulsion between the ligands and the steric geometry of the *N,N',O*-chelate. In addition, the *N,N',O*-chelate contributed to a difference in the C–N(imine)–C bond angles, with the C1–N1–C7 bond angle (127.2°), in which C7 is a part of the phenyl group with the ethoxy substituent coordinated to the Ni center, wider by ca. 3° than the C2–N2–C15 angle (123.1°). Each amine N atom on the outer side of the ligand interacted with O atoms of the counter ClO₄⁻ ion through hydrogen bonding (Table S3), and the C4–N3–C23 and C5–N4–C31 bond angles were similar to one another.



Scheme 3 Isomerized structure of **2c**.

Substituent effect

The influence of the RApH₂ substituent on the properties of the dinuclear complexes **1a–1e** was evaluated by plotting the energy of the MLCT transition and redox potentials to the acid dissociation constant of the precursor aniline derivative (pK_a^R) employed in the synthesis of the corresponding RApH₂ (Figure 3). Both the energy of the MLCT band (**1a**: 17890,¹² **1b**: 17760, **1c**: 17900, **1d**: 18250, **1e**: 18280 cm⁻¹) and the redox potentials decreased as the pK_a^R increased (Figures 3A and 3B, respectively), indicating that the electron density on the metal centers increase as increasing the electron-donating ability of R. Similar trends of the energy of MLCT depending on pK_a^R to the first redox potentials on pK_a^R suggest that the electron-donating ability of the R group in the RApH₂ ligand significantly affects the electronic state of metal ions.

Catalytic polymerization

The polymerization of styrene occurred only in the presence of both **1** and MAO and not in the presence of just **1** or MAO. These results indicate that the active species generated by the addition of MAO to **1** plays a critical role in the catalysis.

Product features. The molecular weights (M_w) and molecular weight distributions (M_w/M_n) of the polystyrene products were only slightly influenced by the Al/Ni ratio but remarkably affected by the temperature (Tables 2 and 3). For example, polymerizations with **1a** at room temperature gave similar products with the values for M_w and M_w/M_n in the range of 28900–35700 and 2.00–2.14, respectively, for Al/Ni ratios varying from 70–1130. However, when the Al/Ni ratio was maintained at 340, a decrease in the molecular weight ($M_w = 33500–13300$) was observed as the temperature increased

(25°C–90°C), while the molecular weight distribution remained within 15% ($M_w/M_n = 2.08–1.75$). These results may be due to increases in the rates of the chain transfer and termination at higher temperatures.¹³

Table 2. Polymerization of styrene with **1a** and MAO.^a

Run	Complex	<i>T</i> /°C	Al/Ni	Conversion (%)	Activity ^b	M_w^c	M_w/M_n
1	1a	25	0	Trace	Trace		
2	1a	25	70	18.9	1.92	3.57	2.07
3	1a	25	110	26.1	2.65	3.18	2.01
4	1a	25	340	31.9	3.24	3.35	2.00
5	1a	25	680	30.0	3.05	3.18	2.03
6	1a	25	1130	31.5	3.20	2.89	2.14

^a Polymerization conditions: reaction time, *t* = 1 h; catalyst condition, [Ni] = 1×10^{-4} mol L⁻¹; styrene addition, 5 mL; solvent, toluene; total volume, 20 mL. ^b 10^5 g PS mol⁻¹ Ni h⁻¹. ^c 10^4 g mol⁻¹.

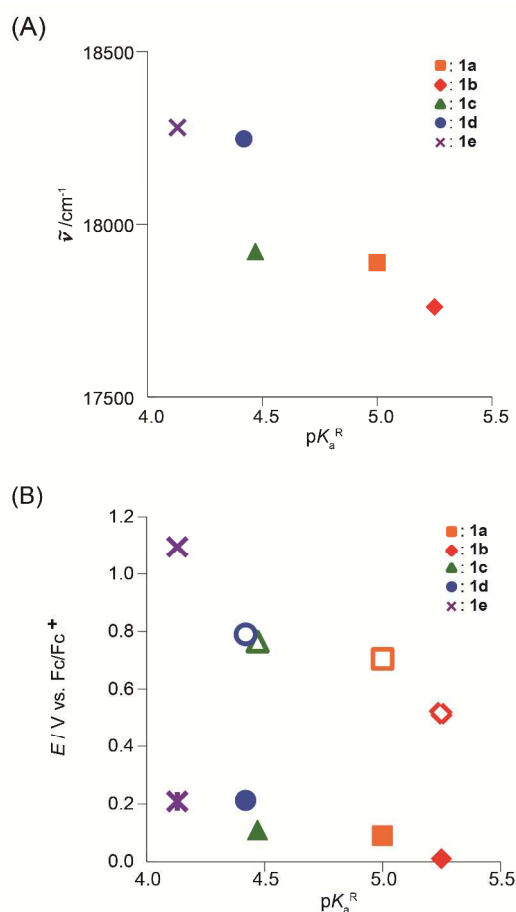


Fig. 3 Dependence of the (A) MLCT energy and (B) redox potentials of **1a–1e** on the pK_a^R of the precursor anilines employed in the syntheses of the corresponding ligand.

Catalytic activity. For the **1a**-MAO catalytic system, runs were performed with Al/Ni = 70, 110, 340, 680, and 1130 at room temperature (Table 2). The activity increased as the Al/Ni ratio increased, and the highest activity of 3.24×10^5 g PS mol⁻¹ Ni h⁻¹ was obtained for Al/Ni = 340 (Run 4 in Table 2). However, at higher Al/Ni ratios, the activity leveled off. These results suggest that a small amount of MAO cannot completely

activate the precatalyst, and the quantity of activated species reaches a maximum above Al/Ni = 340.

The **1a**-MAO system with Al/Ni = 340 showed temperature-dependent catalytic activity (Table 3 and Figure 4). The activities increased with temperature up to 70°C, where the highest activity (6.59×10^5 g PS mol⁻¹ Ni h⁻¹, Run 9) was observed, then slightly decreased at 90°C (6.41×10^5 g PS mol⁻¹ Ni h⁻¹). The effect of temperature on the competition between the formation of the active species or chain transfer and the decomposition of the active species obviously be responsible.

Table 3. Polymerization of styrene with **1a–1e**.^a

Run	Complex	T/°C	Al/Ni	Conversion (%)	Activity ^b	M _w ^c	M _w /M _n
7	1a	50	340	43.9	5.03	2.23	2.00
8	1a	60	340	54.4	5.51	2.81	1.82
9	1a	70	340	65.1	6.59	1.56	1.84
10	1a	90	340	63.2	6.41	1.33	1.86
12	1b	r.t.	340	22.5	2.38	3.42	1.90
13	1b	50	340	43.8	4.43	2.48	2.02
14	1b	60	340	46.5	4.63	2.36	1.86
15	1b	70	340	63.8	6.36	1.50	1.80
17	1c	25	340	36.0	3.61	3.26	2.00
18	1c	50	340	39.4	3.93	2.52	2.08
19	1c	60	340	39.9	3.98	2.47	1.87
20	1c	70	340	39.4	3.93	1.81	1.86
21	1d	25	340	38.4	3.89	2.88	2.00
22	1d	50	340	54.6	5.53	2.57	1.85
23	1d	60	340	64.3	6.51	1.62	1.71
24	1d	70	340	66.7	6.75	2.21	1.75
25	1e	25	340	21.4	2.17	4.34	1.92
26	1e	50	340	39.8	4.03	2.71	1.88
27	1e	60	340	60.3	6.11	2.29	1.93
28	1e	70	340	73.7	7.46	2.08	1.84

^a Polymerization conditions: reaction time, $t = 1$ h; catalyst condition, $[\text{Ni}] = 1 \times 10^{-4}$ mol L⁻¹; styrene addition, 5 mL; solvent, toluene; total volume, 20 mL. ^b 10^5 g PS mol⁻¹ Ni h⁻¹. ^c 10^4 g mol⁻¹.

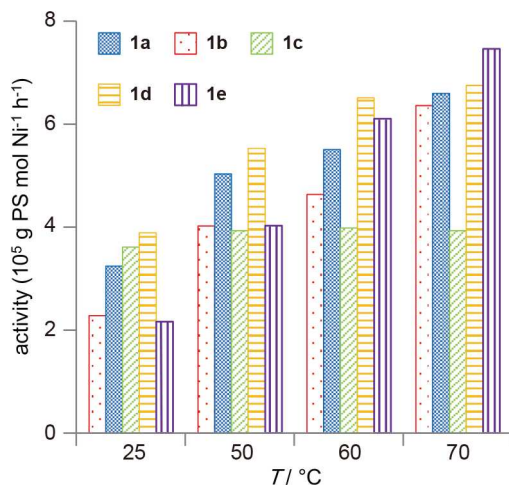


Fig. 4 Temperature dependence of the catalytic activity. Polymerization conditions: reaction duration, $t = 1$ h; catalyst concentration, $[\text{Ni}] = 1 \times 10^{-4}$ mol/L; styrene addition, 5 mL; solvent, toluene; total volume, 20 mL.

The catalytic activities of **1b–e** were also studied at room temperature, 50°C, 60°C, and 70°C. Interestingly, the activities of **1b**, **1d**, and **1e** were found to depend on the temperature in a manner similar to that of **1a**, whereas the activity of **1c**

remained constant in the range of $3.61\text{--}3.98 \times 10^5$ g PS mol⁻¹ Ni h⁻¹, independent of the temperature (Runs 17–20).

The substituent effect in complexes **1a–1e**, except for **1c**, on the activity is illustrated in Figure 5. The catalytic activities of **1a**, **1b**, and **1d** at each room temperature, 50°C, and 60°C decreased as the pK_a^R increased, and the electron-donating ability of R influences on the activity of the metal centers. In fact higher activity is obtained by complexes including active centers with lower electron density. This result is caused by the effect of donating ability of R on the following two events in the catalytic process: i) on coordination of styrene to the metal center through π -donation, suggesting that styrene favors coordination to metal centers with lower electron density; ii) on 2,1-insertion of styrene monomer into the Ni–H and Ni–polymer bonds during chain propagation, indicating that catalyst with higher electron density retards chain propagation by stronger π back-donation. Although the cyclic voltammetry (CV) results indicated a lower electron density of the metal centers in **1e** than that of **1d**, the activities of the former was lower than those of the latter at room temperature, 50°C, and 60°C. The lower activities of **1e** may be induced by steric hindrance near the active centers because four ethyl groups block the coordination of monomers to the metal centers. Note that the activities of **1a**, **1b**, **1d**, and **1e** at 70°C decreased slightly as the pK_a increased, indicating that electronic rather than steric factors influence the polymerization process.

One of the important features of this class of Ni^{II} complexes is the dinuclear structure. It could be possible that there is an effect of the dinuclear structure. However, these catalytic systems showed same order of activities as those of the analogous mononuclear Ni^{II} complexes with N,N' cheating ligands,^{4n,4m,4p} suggesting that the dinuclear effect was little.

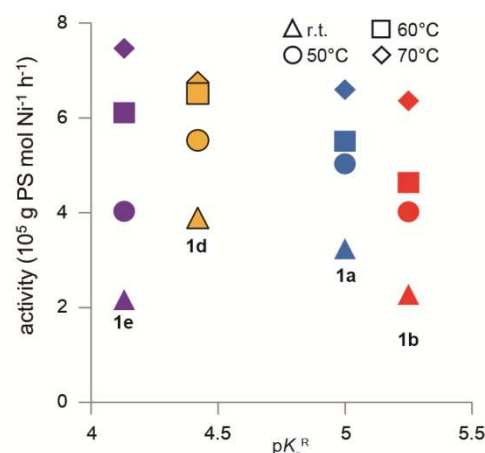


Fig. 5 Relationship between the catalytic activity of **1a**, **1b**, **1d**, and **1e** at various temperatures and the pK_a^R of the precursor anilines employed in the syntheses of the corresponding ligands.

Catalytic polymerization with **1c** at 0°C (1.34×10^5 g PS mol⁻¹ Ni h⁻¹) showed lower activity than activities above 25°C (Table 3). Trend of activity for **1c** is different from those of other catalytic systems, and the unexpected trend may be derived from an retardation of chain propagation. In the precursor complex, each acac^- ligand forms a chelate with a metal center. In the activated species, following the dissociation of an acac^- ligand, one of the oxygen atoms of the ethoxy groups on the ligand predominantly coordinates to the active center, thus retarding the coordination of styrene molecules. The X-ray crystallographic analysis of **2c** clarified that 2-OEtApH₂

behaves as an *N,N',O* chelating ligand of the Ni center (Figure 2B).

The polystyrene samples obtained using all the different complexes were determined to be atactic polystyrenes by their ^{13}C NMR spectra, which showed a broad signal in the range of δ 146–145 assigned to the aromatic C-1 resonance (Figure 6). The stereo-triad distribution for each atactic polystyrene was calculated from the integrated values of the three main peaks of the C-1 resonance: the isotactic (mm), heterotactic (mr), and syndiotactic (rr) triads. The ^{13}C NMR spectrum of the polystyrene obtained at 25°C using the **1a**-MAO catalytic system with Al/Ni = 340 (Run 4) had C-1 resonances at δ 146.0, 145.6, and 145.1, which were assigned to the mm, mr, and rr triads, respectively, and the stereo-triad distribution was [mm] = 50.3%, [mr] = 25.6%, and [rr] = 24.1%. The polystyrenes obtained using the other catalytic systems exhibited similar stereo-triads.

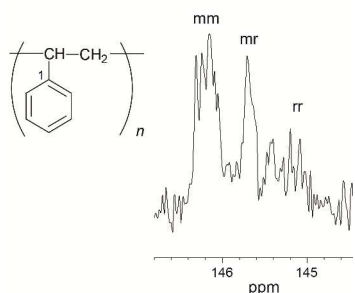


Fig. 6 ^{13}C NMR spectrum (stereo-triad distributions of atactic polystyrene) of polystyrene obtained by **1a**-MAO catalytic system at room temperature.

Finally, the ^{13}C NMR spectra of the polymers also provided information about the polystyrene end groups. The signal at δ 22 is assigned to the methyl carbon formed following the secondary insertion of styrene into the Ni–H bond of the active species during chain initiation. The resonance at δ 137 is assigned to the vinylene carbon in the double bond of the $-\text{CH}=\text{CHPh}$ end group generated via β -H elimination. On the other hand, no resonances could be assigned to the vinyl carbon in the end-group $-\text{CPh}=\text{CH}_2$ or the carbons in the $-\text{CHPh}-\text{CH}_2-\text{CH}_3$ end group. These results suggest that styrene monomer inserts mainly into the Ni–H bond of the active species in a 2,1-fashion during chain propagation, with chain termination occurring via β -H elimination.

Conclusion

Dinuclear and mononuclear Ni complexes **1a–1e** and **2c**, respectively, with azophenine derivatives as ligands were synthesized. The molecular structures of **1b**, **1c**, and **1e** exhibited the delocalization of six π -electrons between the metal centers, and that of **2c** showed *N(imine),N'(imine),O(ethoxy)*-coordination as a result of isomerization from the *para*-benzoquinonediimine form of the free ligand to the *ortho*-benzoquinonediimine form in the complex. The electronic nature of R in **1** enabled the fine tuning of the electronic properties of **1**, and the electron density of the Ni centers increased as the electron-donating ability of R increased. The complexes **1** activated by MAO showed catalytic activity for styrene polymerization, with a maximum activity of 7.46×10^5 g PS mol $^{-1}$ Ni h $^{-1}$ for **1e**. The nuclearity

of the complexes, which was determined by the electron-donating ability of R for **1a**, **1b**, and **1d** and the bulkiness of the ligand backbone for **1e**, influenced on the activity.

Experimental section

Caution!!! Although the perchlorate salts prepared in this study do not appear to be shock sensitive, they should be handled with caution and only in very small quantities.

General Procedures

All manipulations involving air-sensitive and moisture-sensitive compounds were performed under argon atmosphere using Schlenk techniques. Toluene and CH_2Cl_2 were freshly distilled over sodium/benzophenone and CaH_2 , respectively. Styrene (Wako Pure Chemical Co.) was dried over CaH_2 and distilled under vacuum prior to use. MAO diluted in toluene was purchased from Tosoh Chemical Co. and used as received. Other commercially available reagents were purchased and used without further purification. The azophenine derivatives RAPH_2 and dinuclear nickel(II) complexes **1a–e** were prepared according to the literature.¹² ^1H and ^{13}C NMR spectra were recorded in CDCl_3 on Bruker DRX-400, AVANCE-500, and AVANCE-400 spectrometers with $(\text{CH}_3)_4\text{Si}$ ($\delta = 0$) as the internal reference. The FAB mass spectra and MALDI TOF mass spectra were recorded on JEOL JMS-700AM and AutoflexIII Bruker mass spectrometers, respectively. UV–vis spectra were recorded on a JASCO V-530 spectrophotometer. The CV was performed in anhydrous CH_2Cl_2 using an ALS Electrochemical System 660A with a platinum working electrode, a platinum counter electrode, and an Ag/Ag^+ (in 0.1 M NBu_4PF_6) reference electrode. The potentials were calibrated in CH_2Cl_2 using the ferrocene–ferrocenium couple (Fc/Fc^+) as an external reference. Gel permeation chromatography (GPC) analyses for the determination of the molecular weights and molecular weight distributions of the obtained polystyrene samples were performed on a JASCO LC-2000 Plus series GPC system using a RI-2031 Plus detector with tetrahydrofuran as the eluent at 40°C and a polystyrene standard as the reference.

Polymerization of Styrene.

All polymerizations were performed under argon atmosphere. A typical polymerization procedure is as follows. A nickel complex in toluene (1×10^{-4} mol/L), toluene, and the appropriate quantity of MAO in toluene were added to a Schlenk bottle, and then styrene was added to the well-stirred solution. The total volume of the reaction mixture, which was set to 20 mL, was continuously stirred for 1 h and then quenched by adding an acidic ethanol solution ($V_{\text{ethanol}}:V_{\text{conc.HCl}} = 10:1$). The polystyrene was isolated by filtration, washed with ethanol, and then dried under vacuum.

Preparations of ligands and complexes

***N,N',N'',N'''*-tetra(4-ethoxyphenyl)-2,5-diamino-1,4-benzoquinonediimine** (4-OEtApH_2). A three necked flask was charged with 1,3-bis(2,6-diisopropylphenyl)imidazolium chloride (0.053 g, 0.12 mmol), NaO^tBu (0.009 g, 0.1 mmol), $\text{Pd}(\text{OAc})_2$ (0.011 g, 0.050 mmol), and toluene (30 mL) under argon atmosphere. After stirring the mixture for 20 min at 80°C, 1,2,4,5-tetrabromobenzene (0.982 g, 2.50 mmol), 4-ethoxyaniline (1.191 g, 13.9 mmol), NaO^tBu (0.963 g, 10.0 mmol) and toluene (15 mL) were added. The mixture was stirred at 110°C for 22 h. After cooling to the room

temperature, the resulting mixture was diluted with hexanes, and precipitated products and inorganic residual were collected by filtration. The precipitated compounds were washed successively with MeOH and CH₂Cl₂ to obtain the desired product. Yield: 1.000 g, 65 %. FAB MS (*m/z*): 617 (M + 1). ¹H NMR (CDCl₃): δ 8.11 (s, 2H, NH), 6.96 (dd, 16H, PhH), 6.20 (s, 2H, CH), 4.05 (q, 8H, CH₂), 1.46 (t, 12H, CH₃). UV-vis (CH₂Cl₂), λ_{max} nm (ε/M⁻¹cm⁻¹): 289(34000), 438(20000). Anal. Calcd for C₃₈H₄₀N₄O₄: C, 74.00; H, 6.54; N 9.08%. Found: C, 73.77; H, 6.56; N 8.93%.

N,N',N'',N'''-tetra(2-ethoxyphenyl)-2,5-diamino-1,4-benzoquinonediimine (2-OEtApH₂). The synthetic procedure for 2-OEtApH₂ was similar with that of 4-OEtApH₂ except using *o*-ethoxyaniline. The products were purified by passing through a silica-gel column (eluent: CH₂Cl₂). Yield: 33%. FAB MS (*m/z*): 617 (M + 1). ¹H NMR (CDCl₃): δ 8.70 (2 H, s, NH), 6.91 (16 H, br s, PhH), 6.20 (2H, s, CH), 4.04 (8 H, q, CH₂), 1.37 (12 H, s, CH₃). UV-vis (CH₂Cl₂), λ_{max} nm (ε/M⁻¹cm⁻¹): 271(25000,sh), 293(29000), 404(20000). Elemental analysis: Found: C, 73.94; H, 6.54; N 9.13%. Calcd. for C₃₈H₄₀N₄O₄: C, 74.00; H, 6.54; N 9.08%.

N,N',N'',N'''-tetra(2-ethylphenyl)-2,5-diamino-1,4-benzoquinonediimine (2-EtApH₂). The synthetic procedure for 2-EtApH₂ was similar with that of 4-OEtApH₂ except using *o*-ethylaniline. The products were purified by passing through a silica-gel column (eluent: CH₂Cl₂). Yield: 48%. FAB MS (*m/z*): 554.4 (M + 1). ¹H NMR (CDCl₃): δ 8.33(2 H, s, NH), 7.23-6.91(16 H, m, PhH), 6.05(2 H, s, CH), 2.65(8 H, q, CH₂), 1.22(12 H, t, CH₃). UV-vis (CH₂Cl₂), λ_{max} nm (ε/M⁻¹cm⁻¹): 289(33000), 377(25000). Elemental analysis: Found: C, 82.43; H, 7.27; N, 9.92%. Calcd. for C₃₈H₄₀N₄: C, 82.57; H, 7.29; N 10.14%.

N,N',N'',N'''-tetra(2,5-diethylphenyl)-2,5-diamino-1,4-benzoquinonediimine (2,6-Et₂ApH₂). The synthetic procedure for 2,6-Et₂ApH₂ was similar with that of 4-OEtApH₂ except using *o*-diethylaniline. The products were purified by passing through a silica-gel column (eluent: CH₂Cl₂). Yield: 28%. FAB MS (*m/z*): *m/z* = 665.7 (M + 1). ¹H NMR (CDCl₃): δ 7.85(2 H, s, NH), 7.03(12 H, s, PhH), 4.61(2 H, s, CH), 2.47(16 H, m, CH₂), 1.13(24 H, t, CH₃). UV-vis (CH₂Cl₂), λ_{max} nm (ε/M⁻¹cm⁻¹): 272(16000), 341(31000, sh), 355(36000). Elemental analysis: Found: C, 83.09; H, 8.49; N, 8.43%. Calcd. for C₄₆H₅₆N₄: C, 83.08; H, 8.74; N 8.29%.

[{Ni(acac)}₂(μ-4-OEtAp)] (1b). Ni(acac)₂ (0.051 g, 0.199 mmol) in CH₂Cl₂ was added to a solution of ligand 4-OEtApH₂ (0.062 g, 0.099 mmol) in CH₂Cl₂. The brown-red color of the solution turned immediately intense purple. The reaction mixture was stirred at room temperature for 30 minutes. After the solvent was removed under reduced pressure, the residue was recrystallized from CHCl₃ adding hexane to obtain a purple crystal. Yield: 0.0518 g, 56.0%. MALDI TOF MS (*m/z*): 931.27 (M + 1); ¹H NMR (CDCl₃): δ 6.64 (16 H, dd, PhH), 5.12 (2 H, s, CH-acac), 4.39 (2 H, s, CH), 3.80 (8 H, q, CH₂), 1.22 (24 H, m, CH₃). UV-vis (CH₂Cl₂), λ_{max} nm (ε/M⁻¹cm⁻¹): 252(56000), 316(23000, sh), 524(22000, sh), 565(29000). Elemental analysis: Found: C, 61.74; H, 5.51; N 5.91%. Calcd. for C₄₈H₅₂N₄Ni₂O₈: C, 61.97; H, 5.63; N 6.02%.

[{Ni(acac)}₂(μ-2-OEtAp)] (1c). The synthetic procedure for 1c was the similar with that of 1b except using 2-OEtApH₂. Yield: 60%. MALDI TOF MS (*m/z*): 931.27 (M + 1). ¹H NMR (CDCl₃): δ 6.99 – 6.88 (8 H, m, PhH), 6.70 – 6.61 (8 H, m, PhH), 5.01 (2 H, s, CH-acac), 4.15 (2 H, s, CH), 4.02 (8 H, q, CH₂), 1.53(12 H, t, CH₃), 1.26(12 H, s, CH₃-acac). UV-vis

(CH₂Cl₂), λ_{max} nm (ε/M⁻¹cm⁻¹): 256(52000), 337(18000), 518(22000, sh), 558(28000). Elemental analysis: Found: C, 61.99; H, 5.65; N 5.84%. Calcd. for C₄₈H₅₂N₄Ni₂O₈: C, 61.97; H, 5.63; N 6.02%.

[{Ni(acac)}₂(μ-2-EtAp)] (1d). The synthetic procedure for 1d was the similar with that of 1b except using 2-EtApH₂. Yield: 63%. MALDI TOF MS (*m/z*): 866.3 (M + 1). ¹H NMR (CDCl₃): δ 6.90(16 H, m, PhH), 5.06(2 H, s, CH-acac), 3.78(2H, m, CH), 2.86(8 H, m, CH₂), 1.30(12 H, m, CH₃), 1.21(12 H, s, CH₃-acac). UV-vis (CH₂Cl₂), λ_{max} nm (ε/M⁻¹cm⁻¹): 247(80000), 326(28000, sh), 473(20000, sh), 509(39000, sh), 548(49000). Elemental analysis: Found: C, 66.44; H, 5.96; N 6.20%. Calcd. for C₄₈H₅₂N₄Ni₂O₄: C, 66.55; H, 6.05; N 6.57%.

[{Ni(acac)}₂(μ-2,6-Et₂Ap)] (1e). The synthetic procedure for 1e was the similar with that of 1b except using 2,6-Et₂ApH₂. Yield: 74%. MALDI TOF MS (*m/z*): 977.5 (M + 1). ¹H NMR (CDCl₃): δ 6.84(14 H, m, PhH), 5.02(2H, s, CH-acac), 3.56(2 H, s, CH), 2.85(8 H, q, CH₂), 1.38(12 H, t, CH₃), 1.16(12 H, s, CH₃-acac). UV-vis (CH₂Cl₂), λ_{max} nm (ε/M⁻¹cm⁻¹): 249(66000), 327(28000), 472(16000, sh), 512(32000), 547(40000). Elemental analysis: Found: C, 68.64; H, 7.01; N 5.82%. Calcd. for C₅₆H₆₈N₄Ni₂O₄: C, 68.73; H, 7.00; N 5.73%.

[Ni(2-OEtApH₂)₂](ClO₄)₂ (2c) The solution of Ni(ClO₄)₂·6H₂O (0.015 g, 0.040 mmol) in MeOH was added to a solution of 2-OEtApH₂ (0.039 g, 0.080 mmol) in CH₂Cl₂, and stirred for 15 min at room temperature. The solvent was removed under reduced pressure and the product was recrystallized with CH₂Cl₂ and hexane. Yield: 0.014 g (66%). UV-vis (CH₂Cl₂), λ_{max} nm (ε/M⁻¹cm⁻¹): 271(57800), 283(54600, sh), 497(50000), 663(14500). Elemental analysis: Found: C 60.49, H 5.34, N 7.28%. Calcd. for C₇₆H₈₀Cl₂N₈NiO₁₆: C 61.22, H 5.41, N 7.52%.

Acknowledgements

This work was supported by Grant-in-Aid for Scientific Research(C) (23510115 to T.F.) from the Japan Society for the Promotion of Science (JSPS). We thank Enago (www.enago.jp) for the English language review.

Notes and references

^a Department of Chemistry, Graduate School of Science and Engineering, Saitama University, 255 Shimo-Okubo, Sakura-ku, Saitama 338-8570, Japan.

^b Comprehensive Analysis Center for Science, Saitama University, 255 Shimo-Okubo, Sakura-ku, Saitama 338-8570, Japan.

† Electronic supplementary information (ESI) available. CCDC 1023073, (2-OEtApH₂); 1023072, (2-EtApH₂); 1023074, (2,6-Et₂ApH₂); 1023068, (1b); 1023069, (1c); 1023070, (1e); 1023071, (2c). For crystallographic data in CIF or other electronic format see DOI: 10.1039/b000000x/

- G. Natta, P. Pino, P. Corradini, F. Danusso, E. Mantica, G. Mazzanti and G. Moraglio, *J. Am. Chem. Soc.* 1955, **35**, 1708.
- (a) N. Ishihara, T. Seimiya, M. Kuramoto and M. Uoi, *Macromolecules*, 1986, **19**, 2464; (b) A. Zambelli, P. Longo, C. Pellecchia and A. Grassi, *Macromolecules*, 1987, **20**, 2035; (c) W. Kaminsky, S. Lenk, V. Scholz, H. W. Roesky and A. Herzog, *Macromolecules*, 1997, **30**, 7647; (d) H. Hagen, J. Boersma, M. Lutz, A. L. Spek and G. v. Koten, *Eur. J. Inorg. Chem.*, 2001, 117; (e) M. Bhattacharjee and B. N. Patra, *Polymer*, 2004, **45**, 3111; (f) M. E. G.

- Skinner, T. Toupance, D. A. Cowhig, B. R. Tyrrell and P. Mountford, *Organometallics*, 2005, **24**, 5586; (g) S. Tobisch, *Chem. Eur. J.*, 2005, **11**, 3113; (h) Y. Choi and J. B. P. Soares, *Polymer*, 2010, **51**, 4713; (i) B. Gao, W. Gao, Q. Wu, X. Luo, J. Zhang, Q. Su and Y. Mu, *Organometallics*, 2011, **30**, 5480; (j) L. E. N. Allan, E. D. Cross, T. W. Francis-Pranger, M. E. Hanhan, M. R. Jones, J. K. Pearson, M. R. Perry, T. Storr and M. P. Shaver, *Macromolecules*, 2011, **44**, 4072; (k) S. K. De and M. Bhattacharjee, *Poly. Chem.* 2011, **49**, 3920.
- 3 L. K. Johnson, C. M. Killian and M. Brookhart, *J. Am. Chem. Soc.*, 1995, **117**, 6414.
- 4 (a) J. Feldman, A. J. McLain, A. Parthasarathy, W. J. Marshall, J. C. Calabrese and S. D. Arthur, *Organometallics*, 1997, **16**, 1514; (b) L. S. Boffa and B. M. Novak, *Chem Rev.*, 2000, **100**, 1479; (c) D. Walther, T. Döhler, N. Theyssen and H. Görls, *Eur. J. Inorg. Chem.*, 2001, 2049; (d) D. Walther, T. Döhler, N. Theyssen and H. Görls, *Eur. J. Inorg. Chem.*, 2001, 2049; (e) V. C. Gibson, A. Tomov, D. F. Wass, A. J. P. White and D. J. J. Williams, *Chem. Soc. Dalton Trans.*, 2002, 2261; (f) L. Bourget-Merle, M. F. Lappert and J. R. Severn, *Chem. Rev.*, 2002, **102**, 3031; (g) D. Zang and G.-X. Jin, *Organometallics*, 2003, **22**, 2851; (h) D. Zhang, G.-X. Jin, L.-H. Weng and F. Wang, *Organometallics*, 2004, **23**, 3270; (i) M. Bialek, H. Cramail, A. Deffieux and S. M. Guillaume, *Eur. Polym. J.*, 2005, **41**, 2678; (j) K. Yliheikkilä, K. Lappalainen, P. M. Castro, K. Ibrahim, A. Abu-Surrah, M. Leskelä and T. Repo, *Eur. Polym. J.*, 2006, **42**, 92; (k) D. Meinhard, M. Wegner, G. Kipiani, A. Hearley, P. Reuter, A. Fischer, O. Marti and B. Rieger, *J. Am. Chem. Soc.*, 2007, **129**, 9182; (l) R. K. O'Reilly, M. P. Shaver, V. C. Gibson and A. J. P. White, *Macromolecules*, 2007, **40**, 7441; (m) H. Gao, L. Pei, K. Song and Q. Wu, *Eur. Polym. J.*, 2007, **43**, 908; (n) Y. Li, M. Gao and Q. Wu, *Appl. Organometal. Chem.*, 2008, **22**, 659; (o) T. Sun, Q. Wang and Z. Fan, *Polymer*, 2010, **51**, 3091; (p) L. Li, C. S.B. Gomes, P. S. Lopes, P. T. Gomes, H. P. Diogo and J. R. Ascenso, *Eur. Polym. J.*, 2011, **47**, 1636; (q) X.-C. Shi and G.-X. Jin, *Organometallics*, 2012, **31**, 4748; (r) Y.-L. Qiao and G.-X. Jin, *Organometallics*, 2013, **32**, 1932; (s) Q. Xing, K. Song, T. Liang, Q. Liu, W.-H. Sun and C. Redshaw, *Dalton Trans.*, 2014, **43**, 7830.
- 5 D. Walther, T. Döhler, N. Theyssen and H. Görls, *Eur. J. Inorg. Chem.*, 2001, 2049; (b) Y.-y. Wang, B.-x. Li, F.-m. Zhu, H.-y. Gao and Q. Wu, *J. Appl. Polym. Sci.*, 2011, **122**, 545; (c) Y. Guo, P. Ai, L. Han, L. Chen, B.-G. Li and S. Jie, *J. Organomet. Chem.*, 2012, **716**, 222; (d) M. R. Radlauer, M. W. Day and T. Agapie, *Organometallics*, 2012, **31**, 2231; (e) L. Zhu, Z.-S. Fu, H.-J. Pan, W. Feng, C. Chen and Z.-Q. Fana, *Dalton Trans.*, 2014, **43**, 2900.
- 6 D. Takeuchi, Y. Chiba, S. Takano and Kohtaro Osakada, *Angew. Chem. Int. Ed.*, 2013, **52**, 12536.
- 7 L. Zhu, Z.-S. Fu, H.-J. Pan, W. Feng, C. Chen and Z.-Q. Fan, *Dalton Trans.*, 2014, **43**, 2900–2906.
- 8 (a) C. Kimish, *Ber. Dtsch. Chem. Ges.*, 1875, **8**, 1026; (b) J. R. Merchant, G. Martyres and N. M. Shinde, *Bull. Chem. Soc.*, 1984, **57**, 1405. (c) K. Ohno, H. Maruyama, T. Fujihara and A. Nagasawa, *Acta Cryst.* 2014, **E70**, o.303; (d) K. Ohno, T. Fujihara and A. Nagasawa, *Acta Cryst.* 2014, **E70**, o.495
- 9 J. Rall, A. F. Stange, K. Hübler and W. Kaim, *Angew. Chem. Int. Ed.*, 1998, **37**, 2681.
- 10 (a) O. Siri, P. Braunstein, M.-M. Rohmer, M. Bénard and R. Welter, *J. Am. Chem. Soc.*, 2003, **125**, 1; (b) T. Wenderski, K. M. Light, D. Ogrin, S. G. Bottc and C. J. Harlan, *Tetrahedron Lett.*, 2004, **45**, 6851; (c) Q.-Z. Yang, O. Siri, H. Brissetb and P. Braunstein, *Tetrahedron Lett.*, 2006, **47**, 5727.
- 11 (a) O. Siri and P. Braunstein, *Chem. Commun.*, 2000, 2223; (b) P. Braunstein, A. Demessence, O. Siri and J.-P. Taquet, *C. R. Chimie*, 2004, **7**, 909; (c) S. Frantz, J. Rall, I. Hartenbach, T. Schleid, S. Zalis and W. Kaim, *Chem. Eur. J.*, 2004, **10**, 149; (d) O. Siri, J.-p. Taquet, J.-P. Collin, M.-M. Rohmer, M. Bénard and P. Braunstein, *Chem. Eur. J.*, 2005, **11**, 7247; (e) J.-p. Taquet, O. Siri and P. Braunstein, *Inorg. Chem.*, 2006, **45**, 4668; (f) O. Siri, P. Braunstein, J.-p. Taquet, J.-p. Collin and R. Welter, *Dalton Trans.*, 2007, 1481; (g) Y.-B. Huang, G.-R. Tang, G.-Y. Jin and G.-X.; Jin, *Organometallics*, 2008, **27**, 259; (h) S. Krupski, J. V. Dickschat, A. Hepp, T. Pape and F. E. Hahn, *Organometallics*, 2012, **31**, 2078; (i) Y. Su, Y. Zhao, J. Gao, Q. Dong, B. Wu and X.-J. Yang, *Inorg. Chem.*, 2012, **51**, 5889; (j) D. Schweinfurth, M. M. Khusiyarov, D. Bubrin, S. Hohloch, C.-Y. Su and B. Sarkar, *Inorg. Chem.*, 2013, **52**, 10332; (k) I.-R. Jeon, J. G. Park, D. J. Xiao, T. D. Harris, *J. Am. Chem. Soc.*, 2013, **135**, 16845; (l) N. Deibel, M. G. Sommer, S. Hohloch, J. Schwann, D. Schweinfurth, F. Ehret and B. Sarkar, *organometallics*, 2014, dx.doi.org/10.1021/om500035c.
- 12 K. Ohno, T. Fujihara and A. Nagasawa, *Polyhedron*, 2014, **81**, 715.
- 13 (a) H. Gao, L. Pei, K. Song and Q. Wu, *Eur. Polym. J.*, 2007, **43**, 908; (b) S. Yu, X. He, Y. Chen, Y. Liu, S. Hong and Q. Wu, *Appl. Polym. Sci.*, 2007, **105**, 500-509.